ELSEVIER

Journal of Structural Geology 26 (2004) 807–824

JOURNAL OF STRUCTURAL GEOLOGY

www.elsevier.com/locate/jsg

Uplift and contractional deformation along a segmented strike-slip fault system: the Gargano Promontory, southern Italy

Charles M. Brankman*, Atilla Aydin

Rock Fracture Project, Department of Geological and Environmental Sciences, Stanford University, Stanford, CA 94305-2115, USA

Received 30 April 2003; received in revised form 28 May 2003; accepted 9 August 2003

Abstract

The Gargano Promontory in southern Italy is a region of localized uplift and contractional deformation within the Apulian foreland province. Our field mapping has defined two main fault systems that controlled the uplift of the Gargano block. E–W-trending strike-slip faults bound the northern and southern margins of the uplifted block, defining a compressive stepover zone between the two fault zones. The second system strikes NW–SE with primarily reverse to oblique-reverse displacements. Uplift was accommodated by a broad antiformal fold and reverse motion on the NW–SE fault system. This deformation is attributed to localized high compressive stress within the stepover region, driven by slip on the bounding strike-slip faults. Three-dimensional numerical models incorporating the observed fault geometries and slip sense support our interpretation. Results show that significantly higher compressive stresses occur within the fault overstep region, and computed stress trajectories agree closely with the orientations of contractional features observed in the field. Although the role of strike-slip faulting in the deformation of the Gargano Promontory has been proposed previously, this mechanism provides a new model for the localized uplift and related deformation. We also cite similar occurrences of this mechanism in the complexly deformed interior of the Apennine fold–thrust belt.
© 2004 Elsevier Ltd. All rights reserved.

Keywords: Gargano Promontory; Strike-slip faults; Mechanical models; Fault segmentation

1. Introduction

In this contribution we describe an example of regional deformation associated with a segmented crustal scale strike-slip fault system. We present field data that shows that the Gargano Promontory, a large block of the Apulian foreland in southern Italy, has been locally uplifted and subjected to contractional deformation as a result of slip along a regional strike-slip fault system, and specifically due to the interaction between échelon segments of this fault system. We support this interpretation with a simple three-dimensional numerical model aimed at reconstructing the observed fault geometries and kinematic relationships. Our goal is to improve the understanding of the mechanism responsible for the Gargano uplift and of the spatial and temporal relationships among the structures involved in the deformation. In addition, we are interested in quantifying the deformation related to the fault system on the regional scale, with an eye to applying this knowledge to subsurface cases of economic interest and surface cases in regions of complex deformation.

2. Regional geologic setting

The Gargano Promontory is located along the eastern coast of southern Italy, extending eastward into the Adriatic Sea away from the otherwise northwest-trending Italian coastline (Fig. 1). The Gargano is a structural block within the Apulian platform, a tectono-stratigraphic domain that forms the foreland and footwall units of the southern Apennine fold-and-thrust belt. The Apulian platform is comprised of a thick sequence of shallow water platform carbonate units that were deposited throughout the Mesozoic and early Tertiary on a passive margin setting related to the opening of the Tethys Sea (Channel et al., 1979). The Apennines formed as a result of N–E vergent thrusting, beginning in the early Miocene, which emplaced a series of

* Corresponding author. Present and corresponding address: Department of Earth & Planetary Sciences, Harvard University, 20 Oxford Street, Cambridge, MA 01238 USA.

E-mail address: brankman@fas.harvard.edu (C.M. Brankman).

0191-8141/$ - see front matter © 2004 Elsevier Ltd. All rights reserved.
doi:10.1016/j.jsg.2003.08.018

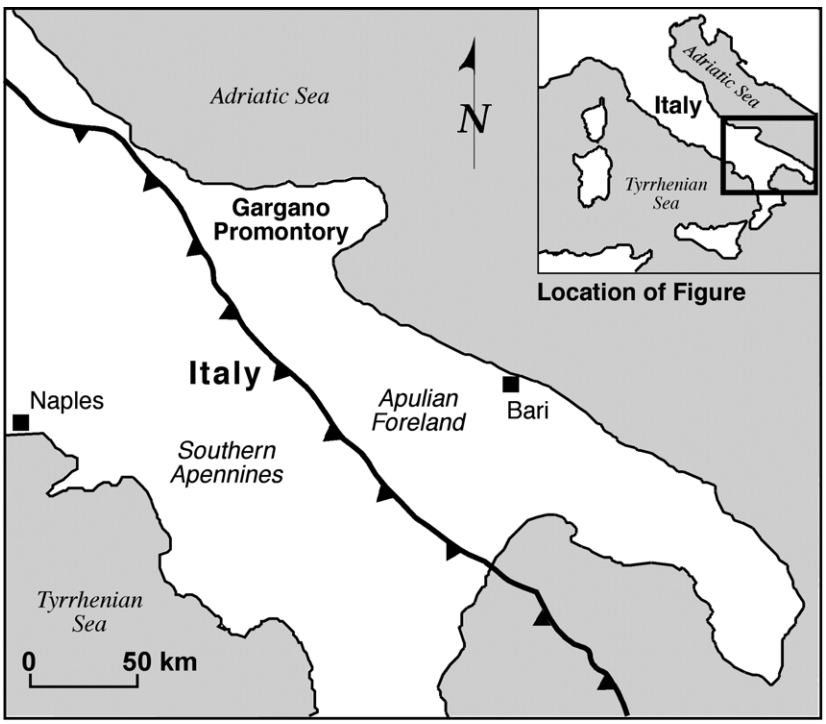

Fig. 1. Overview and location map of southern Italy, showing locations of the Apulian Foreland, southern Apennines, and the Gargano Promontory.

thick Mesozoic and early Cenozoic carbonate platform (Apenninic platform) and deep water basinal units (Lagonegro–Molise and Liguride units) onto the western margin of the Apulian platform. This compressive event lasted through the late Pliocene, and resulted in a large-scale duplex system within the allochthonous units and imbrication of the overthrusted Apulian units (Cello et al., 1989; Patacca and Scandone, 1989; Patacca et al., 1990). A NE–SW oriented extensional deformation has since overprinted the compressive structures (Amato et al., 1995).

The Gargano Promontory (Fig. 2), the region considered in this study, is located in the foreland of the Apennines, about 50 km east of the thrust front. The Apulian foreland forms a broad, low elevation region east of the Apennines, and exhibits very low levels of deformation with respect to the interior of the Apennines. The foreland exhibits primarily extensional deformation, with NW–SE striking normal faults dividing the region into a series of fault blocks (Funiciello et al., 1991; Marsella et al., 1995). In contrast, the Gargano Promontory is a 1000 km^2 region which has been uplifted to 900 m above the adjacent foreland. Geologic and geophysical data indicate that the Gargano is a region of local crustal uplift and anomalous contractional deformation within the relatively less deformed Apulian foreland. Gravity surveys have revealed a positive Bouguer gravity anomaly of 110 mGal coinciding with the location of the Gargano uplift (Finetti and Morelli, 1973). Similarly, the depth to magnetic basement, inferred from aeromagnetic surveys (Cassano et al., 1986), is about 8 km as compared with 10 km or deeper in the adjacent foreland region and offshore Adriatic. The Gargano and adjacent offshore Adriatic is a region of active seismicity, with several recent seismic sequences with event magnitudes up to 5.3 (Favali et al., 1990, 1993b; Console et al., 1993).

While the above data indicate that the Gargano is a distinct structural block from the remainder of the foreland, relatively few studies have focused on the structural evolution of the region. Several authors (e.g. Finetti et al., 1987; Favali et al., 1990) have incorporated the Gargano block into geodynamical models of the Adriatic and the circum-Mediterranean region, but have not characterized the detailed internal structure of the Gargano block. The few structural studies focusing on the Gargano vary greatly in their structural interpretations and conclusions. Ortolani and Pagliuca (1987) proposed that the Gargano block was uplifted along E–W-trending, south-vergent reverse faults, and that the uplift was due to compressional tectonics related to the Dinarides north and east of the Adriatic. Argnani et al. (1993) examined the offshore Adriatic Sea east of the Gargano using marine seismic data, and proposed that uplift occurred as the result of inversion of pre-existing normal faults due to Dinaride compression. Funiciello et al. (1988, 1991) and Favali et al. (1993a) concluded that the structural evolution of the Gargano incorporated multiple episodes of deformation, including extensive strike-slip and normal faulting, and block rotation. However, much of the detailed structural analyses have focused on the region adjacent to the southern margin of the uplifted block, and do not analyze in detail the interior of the region.

A common feature of previous structural studies in this area is the incorporation of several successive episodes of deformation to account for the uplift of the Gargano block

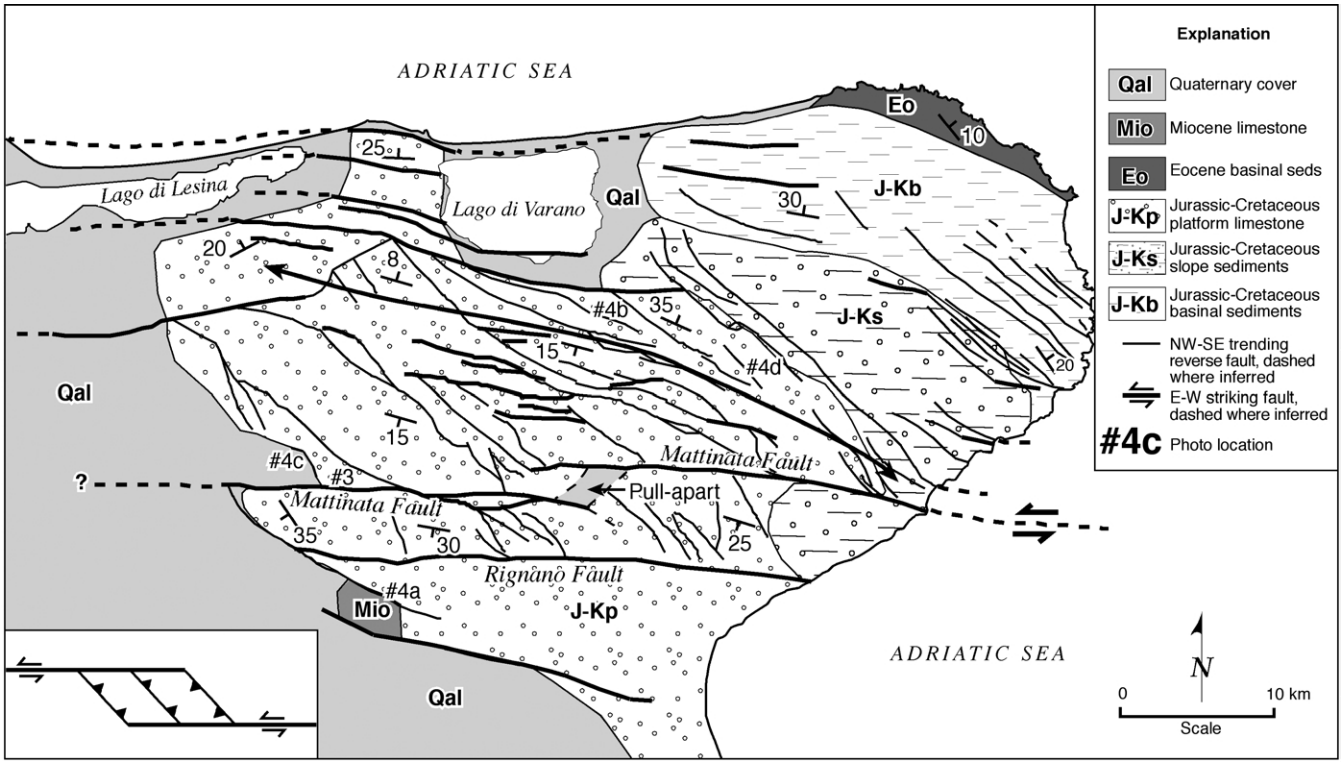

Fig. 2. Fault map of the Gargano Promontory, southern Italy. Faults traces are from field mapping, interpretation of aerial photographs, and modified from Carta Geologica d'Italia, Foglio 155, 156, 157, 164 (Martinis and Pavan, 1967; Merla et al., 1969; Boni et al., 1969; Cremonini et al., 1971). The uplifted Gargano block is bounded on the north and south margins by left-lateral strike-slip faults, with numerous NW–SE striking reverse faults in the stepover zone. The apparent right-lateral displacement on the Mattinata fault is a result of topographic relief across the fault (Salvini and Funicello, 1994). Inset shows schematic of fault relationships. Numbers represent location of photographs in Figs. 3 and 4.

and the structures therein. We describe below a simple model that accounts for the deformation and uplift of the Gargano structural block. Our hypothesis is that deformation was controlled by left-lateral strike slip faults that bound the uplifted Gargano block and are arranged in an overlapping, right stepping geometry. This geometry forms a compressional step within which deformation is accommodated by folds and reverse faults. Some aspects of this fault system and its contribution to the deformation of the Gargano have been recognized by previous authors (e.g. Funiciello et al., 1988, 1991; Favali et al., 1993a; Salvini et al., 1999). However, we believe that the specific primary mechanism for the uplift and related deformation, which we propose in this contribution, has not been applied to this region.

3. Methodology

Our field investigations in the Gargano centered on identifying the key structural elements that would reveal the mechanism of uplift in the region. We utilized previously published geologic maps (e.g. Martinis and Pavan, 1967; Boni et al., 1969; Merla et al., 1969; Cremonini et al., 1971) and 1:25,000 scale aerial photographs as base maps for our investigations. After defining the overall structural setting and identifying the different categories of structures, we selected key outcrops for detailed characterization of fault zone structures and shear sense indicators. Because of the limited outcrop exposure in the Gargano, we relied heavily on quarry exposures and roadcuts, as well as the geomorphic expression of fault zone traces, to infer the geometries and kinematics of the fault systems present.

4. Structural features present in the Gargano

On a regional scale, the Gargano uplift defines a gentle anticlinal structure. The axis of the anticline trends roughly N60°W and plunges gently to the northwest in the western part of the region. Dips range from nearly horizontal throughout the broad crest of the structure to about 25° along the southern and western margins (Fig. 2). Locally, however, bedding attitudes show large variations, with dips reaching nearly 80° in some areas. Bedding is especially disrupted and/or dips steeply in the vicinity of large faults.

Two main systems of faults are present throughout the Gargano (see Fig. 2). The first is a set of E–W striking faults which occur primarily at the northern and southern boundaries of the Gargano block. The second is a system of northwest striking faults, which is pervasive across the

entire region. We believe that these two systems of faults are intimately related and are crucial for understanding the origin and the mechanism for the uplift and deformation of the region.

4.1. E–W striking boundary faults

The Gargano block is bounded on the northern and southern margins by E–W striking, left lateral strike slip faults The best known and most closely studied of these structures is the Mattinata fault, which is located along the southern margin of the Gargano uplift. This fault has been described by other workers (Funiciello et al., 1988, 1991; Salvini et al., 1999). The Mattinata fault defines a linear topographic valley that trends due E–W. To the east, the Mattinata fault extends well into the Adriatic Sea, where it is clearly imaged on marine seismic lines for at least 100 km and possibly for several hundred kilometers (de Dominicis and Mazzoldi, 1987; Finetti et al., 1987; Argnani et al., 1993). There is no evidence for the continuation of the Mattinata fault to the west; rather, the fault appears to terminate at the southwestern corner of the uplifted block. The magnitude of slip across the fault has been estimated to be a minimum of 5 km of left-lateral slip, based on the presence of a well-defined pull-apart basin located at a local left step between fault strands (Funiciello et al., 1988, 1991; Favali et al., 1993a; Salvini and Funicello, 1994). Lack of correlatable offset markers does not allow for a more precise determination of slip, but the minimum 5 km left-lateral slip estimate together with a minimum 100-km-length indicates that the structure is a major crustal-scale fault.

At a more detailed scale, the Mattinata fault zone is composed of several subparallel strands that are anastamosing about an overall E–W trend. Exposures in several quarries along the fault allow for detailed observation of the fault zone. The Mattinata fault is characterized by a localized fault core of highly brecciated rock 100–200 m wide, within which the limestone present on either side of the fault have been fragmented and brecciated locally to a sand-like consistency (Fig. 3a). Within this fault core are numerous discrete subvertical slip planes with nearly horizontal slickensides (Fig. 3b), which appear to accommodate much of the displacement. Slip plane orientations vary widely within the fault core (Fig. 3c). Brittle deformation associated with the Mattinata fault is extremely localized to the fault core, with no significant damage zone extending outward into the host rock. For example, bedrock in quarries less than 1 km from the Mattinata fault trace are much less fractured, showing almost no notable fault-parallel deformational structures.

In addition to the Mattinata fault, a subparallel fault, the Rignano Fault (Salvini et al., 1999) runs along the southern border, marking a sharp break in slope north of which a large amount of uplift has occurred. A third E–W striking fault is present south of the Rignano Fault; it bounds a slightly uplifted plateau to the north from the lower foreland and is considered the southernmost structure of the southern boundary of the Gargano.

Two defining characteristics of the Mattinata fault are the prominent E–W linear topographic expression of the fault trace, and the extremely brecciated nature of the internal fault core about 100–200 m wide. In areas of poor exposure and limited outcrops, we were able to use these fault zone characteristics to identify faults of similar magnitude.

Similar to the southern boundary faults of the Gargano block, several subparallel northern boundary fault strands can be identified (see Fig. 2) over a broad zone several kilometers wide. Although these faults are neither as prominent nor as well exposed as the Mattinata fault, they display similar characteristics to the Mattinata fault: E–W-trending topographic lineaments and internal fault zone brecciation identical in texture, magnitude, and dimensions to that seen in quarries along the Mattinata fault. We take these similarities as evidence that the northern boundary faults are of similar shear strain or slip magnitude to the Mattinata fault. There is no evidence of the extension of these northern E–W striking faults to the east into the Adriatic Sea, as seismic data does not show any faults along the trend of the northern boundary (Finetti et al., 1987; Argnani et al., 1993). Several workers, however, have postulated the existence of transverse structures in this area extending to the west (e.g. Favali et al., 1993a,b). Lavecchia (1988) shows the Apennine thrust front offset in a left-lateral sense at the latitude of the northern margin of the Gargano uplift (see Fig. 1). The linear geomorphic expression of the northern coast of the Gargano, and its extension to the west, again in an en-échelon fashion, is indicative of a fault-controlled northern boundary. In addition, the existence of localized intrusive igneous bodies along this lineation, which may have been introduced along the fault zone, has been documented (Bigazzi et al., 1996). Such localized intrusions are common along crustal scale strike-slip fault systems (Aydin et al., 1990), and provide further indirect evidence of the extension of these northern bounding strike-slip faults to the west of the Gargano.

4.2. NW–SE striking faults

A second, more pervasive set of faults, striking between N40°W and N70°W, also occurs throughout the Gargano (Fig 2). These faults are manifested more subtly than the dramatic fault zones of the Mattinata fault and associated subparallel structures, but are generally well defined by NW-trending topographic lineaments. These have been mapped as faults by previous workers (e.g. Cremonini et al., 1971; Funiciello et al., 1988), but the details of their kinematics have not been documented in detail. We have identified several locations where the internal fault zone structures are such that the sense of slip can be determined, and in some cases the magnitude of slip can be estimated.

In general, these faults occur as relatively narrow (<10s of meters) zones of highly fractured and brecciated rock.

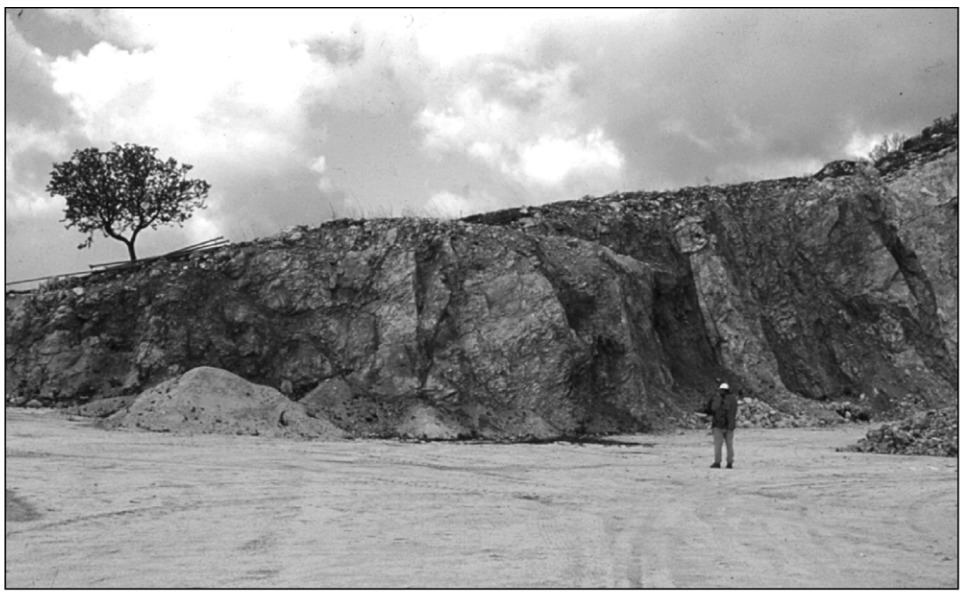

a)

b)

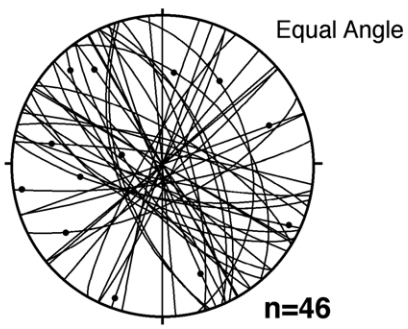

c)

Fig. 3. (a) Quarry exposure of the Mattinata fault, a major E–W-trending strike-slip fault. The quarry exposes the interior of the fault zone, composed of highly brecciated limestone with well defined slip surfaces. View is to the west. (b) Slickensides indicate strike-slip motion on slip planes. (c) Stereonet showing orientations of numerous slip planes within the fault core.

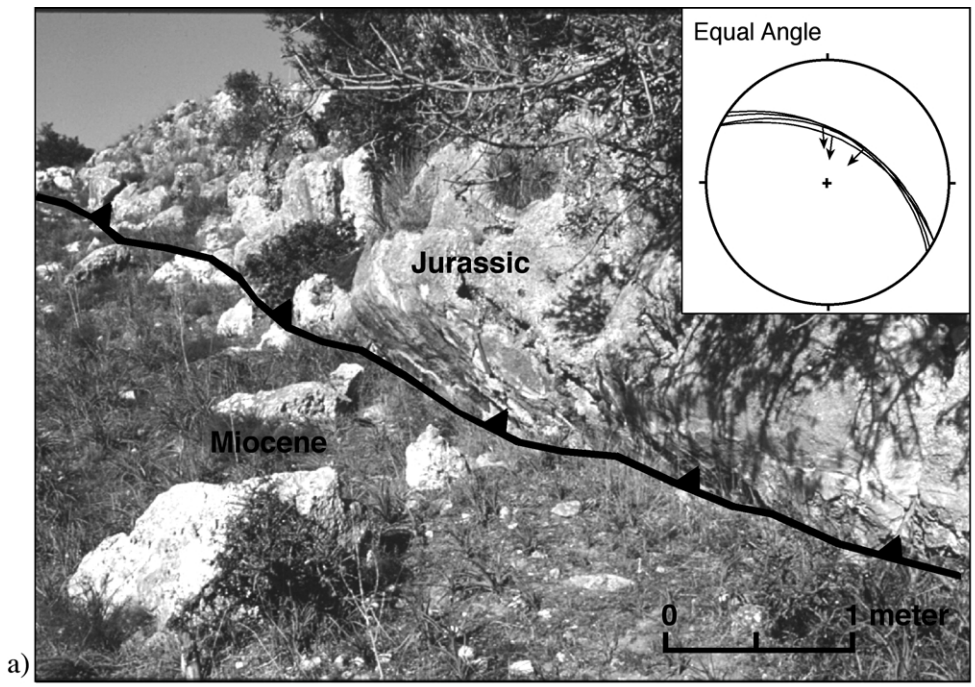

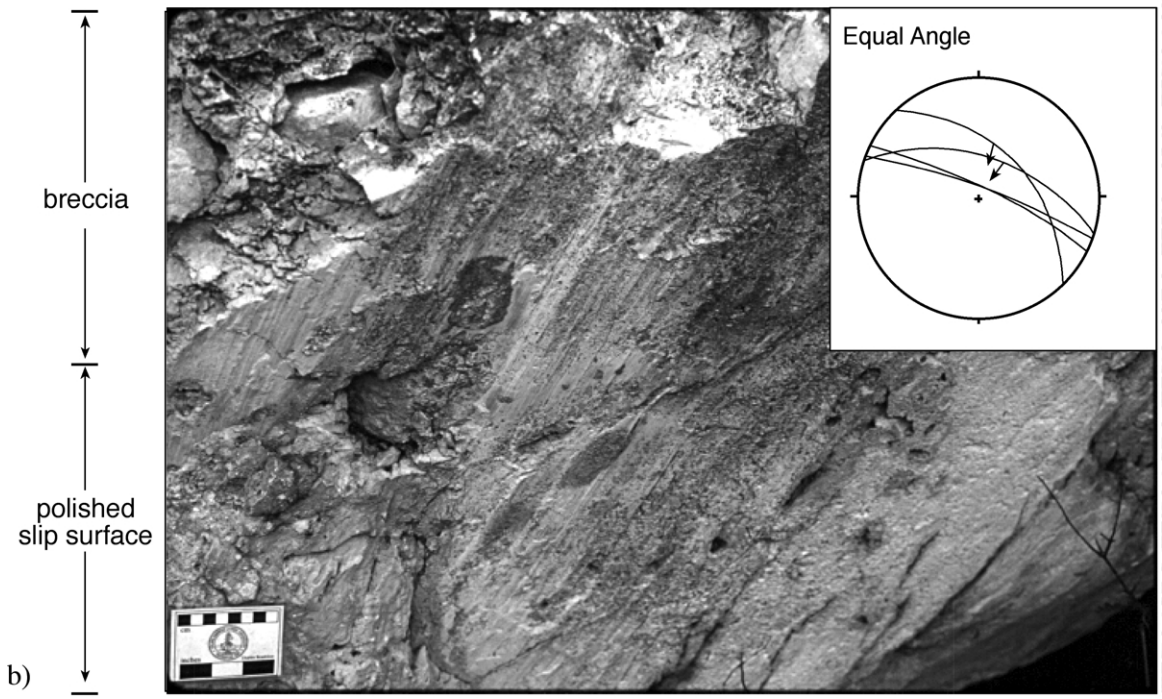

Fig. 4. Fault zone characteristics associated with northwest striking reverse faults. See Fig. 2 for photo locations. (a) Jurassic limestones in reverse fault contact with Miocene basin sediments. View is roughly due north. (b) Detail of slip surface within reverse fault breccia zone, showing nearly dip-slip slickensides. Inset shows orientation of slip surfaces along this fault zone. Lithologic offsets and topography indicate reverse motion on this fault. (c) Quarry exposure of brecciated fault zone along a northwest striking reverse fault. Within the breccia, remnant bedding is offset in a reverse sense along discrete slip surfaces. View is to the southeast. (d) Small reverse fault with about 15 cm of reverse offset. Fault is oriented N50W, 45S. (e) Orientations of tectonic pressure solution surfaces, indicating NE–SW compression within the Gargano block. The presence of contractional structures such as these throughout this area indicates that the Gargano Promontory was subjected to primarily compressional stresses during its deformation and uplift.

c)

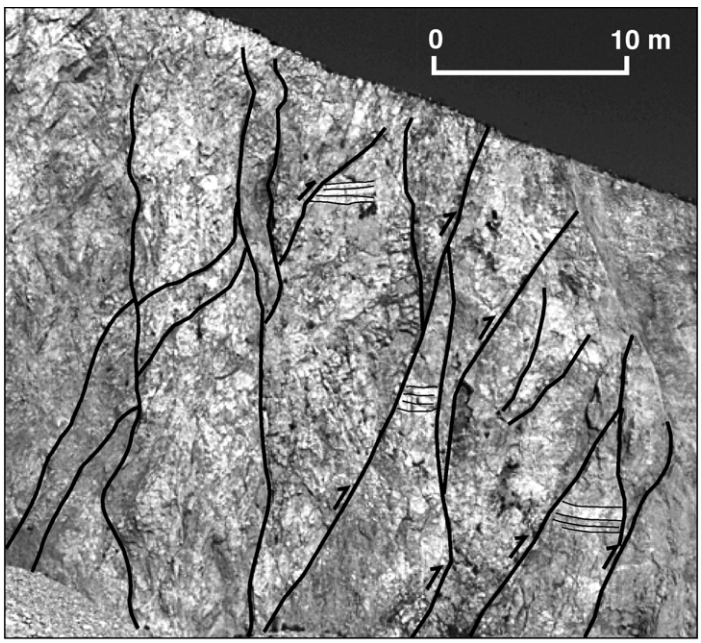

d)

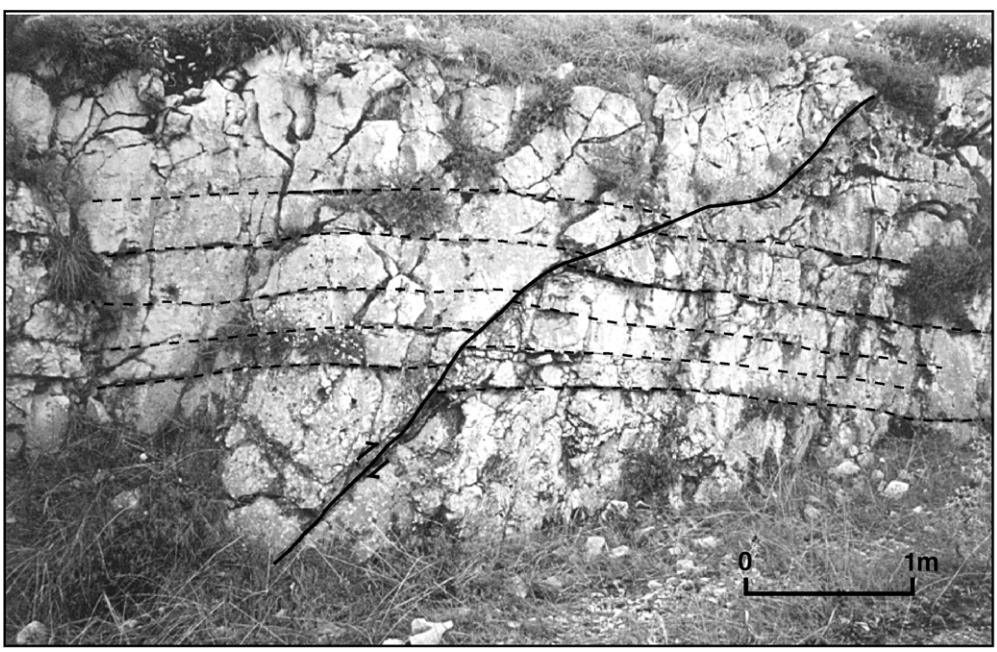

e)

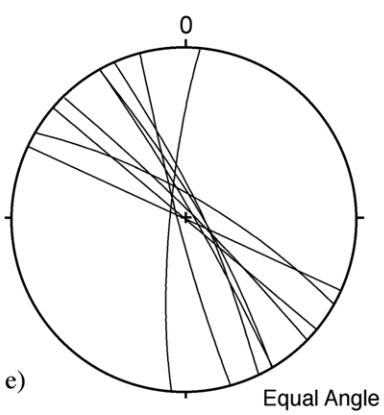

Bedding is highly tilted, fractured, or otherwise disrupted adjacent to the fault zone. In places, however, the fault geometries and lithologic offsets provide clear evidence of the nature of the NW striking faults. Fig. 4a shows an outcrop exposure of hanging wall Jurassic carbonates in reverse contact with Miocene rocks in the footwall. This outcrop, while not in the zone north of the Matinatta Fault, is located within a small uplifted block in a compressional step between the Rignano fault and a subparallel fault to the south, and typifies the style of deformation on the NW-striking faults. The fault zone consists of relatively narrow zones of brecciation localized along the main fault slip plane. The vertical displacement displayed at this outcrop is indicative of the compressional nature of the Gargano and the magnitude of uplift that is accommodated across these NW-striking reverse faults.

Lithologic offsets across these faults are often difficult to determine due to the thick sequences of relatively homogeneous units combined with limited outcrop exposures. However, in a similar manner to that used in the interpretation of the E–W strike-slip faults (see above), we identified examples of fault zones that display similar characteristics and structures to those seen in the well exposed examples such as that shown in Fig. 4. Detailed examination of fault zone structures, such as fault slip planes and associated structures, including slickensides (Fig. 4b), steps along slip surfaces, tail fractures originating on slip surfaces, and clear offset markers (Fig. 4c and d), consistently indicate reverse motion on the NW-striking faults.

4.3. Fault intersection relationships

While there are few locations where the details of the fault intersections and terminations can be observed, in several cases the relationships can be determined from topography or from aerial photos. In all cases where the two fault sets intersect, the NW striking faults either terminate against or merge into the EW faults. The strike-slip faults are not offset by the reverse faults. These key relationships indicate that the NW striking faults are genetically related to, and perhaps driven by, the left-lateral motion on the EW striking faults.

4.4. Stylolitic pressure solution structures

In addition to the reverse faults described above, other contractional structures were observed in the study area Pressure solution seams are one of these types and were found in several locations away from the major fault zones. The seams are oriented nearly vertical with a NW–SE strike, subparallel to the strike of the reverse faults described above (Fig. 4e), and have stylolitic teeth normal to the solution plane. It is well known that stylolitic pressure solution surfaces, distinct from shear-related slickolites, form perpendicular to the greatest compressive principal stress (Fletcher and Pollard, 1981). Therefore, we can use these structures to determine the principal stress orientations at the time of the deformation. The consistent orientation of the stylolitic pressure solution seams indicates that the maximum compressive principal stress was oriented NE–SW. This agrees well with the orientation of the reverse faults mapped in the Gargano Promontory (see above), and provides further evidence of contractional deformation in this region. It should be noted that these tectonic pressure solution structures are distinct from bed-parallel stylolites formed in response to the overburden pressure and compaction that are common throughout the limestone units in the study area. In addition, the stylolitic solution seams recorded in this study are different from what is referred to as the pressure solution cleavage by previous workers (Salvini et al., 1999; Billi, 2003) at least in orientation and spatial distribution; the pressure solution cleavages reported by these workers are parallel and adjacent to the main fault zone and were interpreted to be formed ahead of the propagating tip of the Matinatta Fault.

Taken together, these contractional structures are in contrast to the remainder of the Apulian foreland, which shows predominantly extensional features. The contractional deformation in the Gargano, then, is purely a local feature and is restricted to well-defined push up block.

5. Numerical modeling

We propose that the overstepping, échelon left-lateral strike-slip faults which bound the uplifted block have interacted to produce a contractional overstep zone (push-up block) associated with the bounding strike-slip deformation. Within this zone, deformation, uplift, and shortening were accommodated by the series of reverse faults. In order to aid in this interpretation, we have used a numerical model to test our hypothesis. We used the program Poly3D (Thomas, 1993), a three-dimensional, displacement discontinuity boundary element code which calculates stress, strain, and displacement fields in an isotropic, homogeneous, linear elastic medium with prescribed faults and other discontinuities. Values of stress and displacement are calculated at user-defined observation points and can be used, for example, to analyze the effects of fault slip on stresses and displacements in the vicinity of the fault(s). Poly3D has been used by several other workers to assess the mechanical interaction between segmented normal faults (Willemse et al., 1996; Crider and Pollard, 1998; Kattenhorn and Pollard, 1999; Maerten et al., 1999).

Our model allows us to prescribe boundary conditions which will drive slip on the E–W striking faults in a half-space, and to determine the effect of this slip on the overstep region. We idealize the admittedly complex northern and southern boundaries of the uplifted region as two vertical strike-slip faults, each extending from the free surface of a semi-infinite half space to a depth of 10 km, which is

approximately the depth to the basement in the Apulian foreland as inferred from aeromagnetic surveys and modeling (Cassano et al., 1986). The two faults overlap by 40 km and are separated by 30 km, which approximate the dimensions of the Gargano uplift (Fig. 5).

The earth is idealized as a homogeneous, isotropic, linear elastic medium with material properties appropriate for near surface, upper crustal rocks. A constant far-field stress field is prescribed in such a way as to impose left lateral motion across the boundary faults. We chose a 5:1 ratio between the magnitudes of the maximum (σ_1) and minimum (σ_3) horizontal stresses. This is admittedly an arbitrary designation, though several other workers (e.g. Segall and Pollard, 1980; Ohlmacher and Aydin, 1997) have also used this stress ratio in their numerical models. The effect of this stress ratio was assessed during the modeling, and is discussed below. The faults are modeled with a range of values for the coefficient of friction, ranging from $\mu = 0.0$ to $\mu = 0.9$. The orientation of the stress field (σ_1 and σ_3 directions), defined here by θ measured counterclockwise from the E–W orientation of the faults, is varied through a wide range of angles. Finally, and distinct from previous models, the half space model used here provides an opportunity for a more realistic representation of the upper crust and the faults, and for several depths of observation planes from the surface to several kilometers deep.

We first consider the simple case of frictionless faults, with an observation grid very near the surface of the half space (Fig. 6). Using $\theta = 30°$ as a base case, we find a region of increased mean stress $(\sigma_1 + \sigma_3)/2$, or increased compression, in the overstep region, in general of about 7.5% and up to 20% and more in the vicinity of the fault tips. An examination of the stress trajectories in the overstep zone

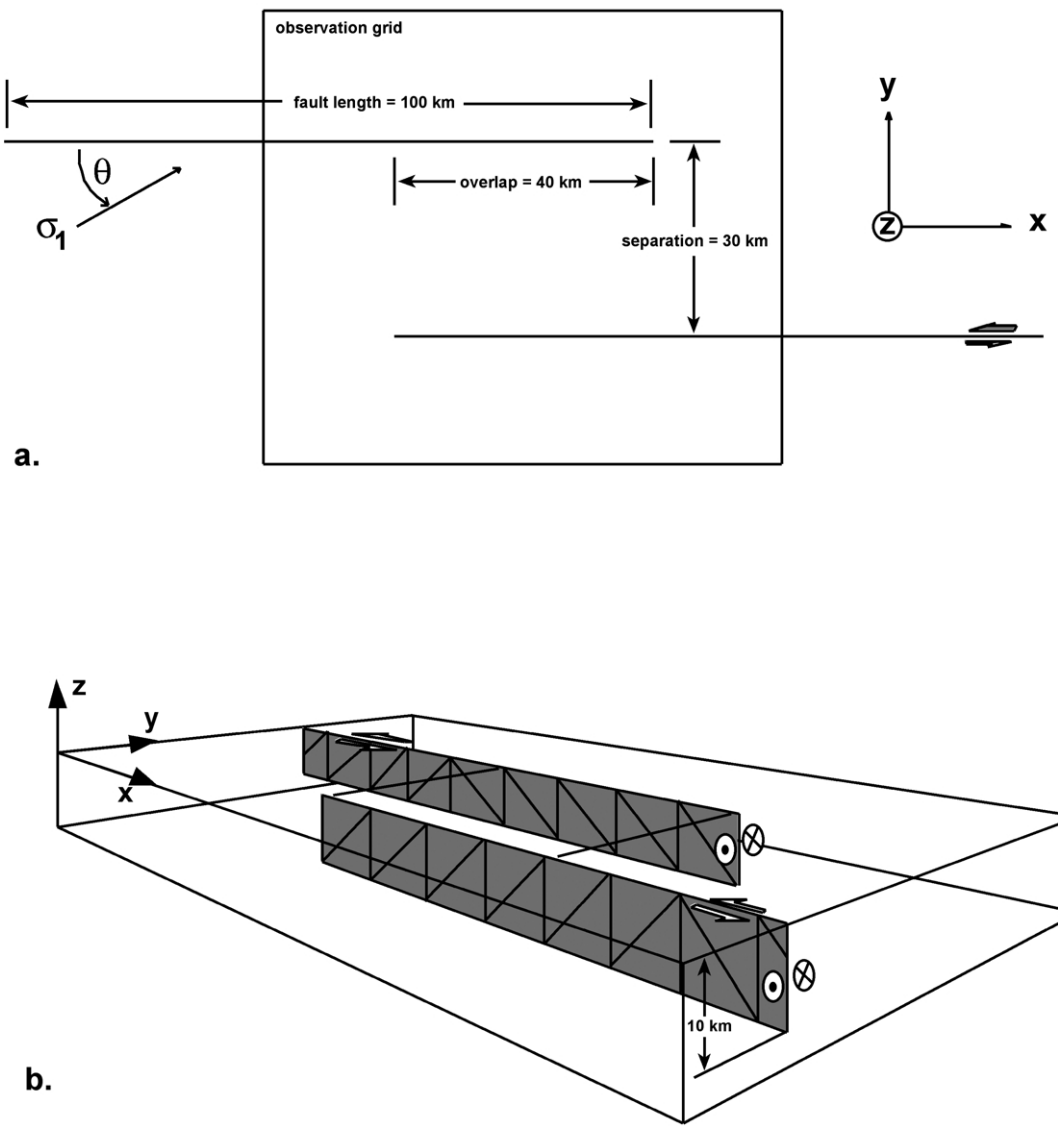

Fig. 5. Schematic Poly3D half-space model configuration. Two vertical left-lateral strike-slip faults are arranged in a right-stepping geometry, which mimics the fault geometry observed in the Gargano Promontory. (a) Map view of model setup. (b) Perspective view towards the northwest.

allows us to determine the orientations of those planes that are perpendicular to the direction of maximum compression, i.e. the strike of contractional features that would form in the resolved stress field. The results show that the contractional structures away from the fault traces would form with orientations of about N30°W, or nearly perpendicular to the far-field maximum compressive stress. Significant deviations from this orientation occur locally along the fault segments, where the frictionless fault surfaces act as principal stress planes and the strike of compressional structures becomes about perpendicular to the fault planes.

Varying the far field stress orientations with respect to the E–W faults (θ) changes both the magnitude and extent of the zone of increased compression between the bounding fault segments, as well as the orientation of resulting contractional structures in the overstep zone. The maximum size of the compressive region is found with $\theta = 45°$; this also corresponds to the highest values of increased mean stress in the overstep zone. Values of $\theta = 15°$ and $\theta = 75°$ correspond to very localized areas of increased mean stress clustered around the fault tips with little interaction between the fault segments (Fig. 7). The orientations of the computed planes of contractional structures are affected primarily by the orientation of the far-field stresses. Only small deviations occur near the fault planes, where the calculated orientations of the planes become either parallel or perpendicular to the fault planes, for θ values of 15° and 75°, respectively.

The effect of frictional faults was assessed using models incorporating a Mohr–Coulomb criterion with constant coefficients of friction in a manner described by Kattenhorn and Pollard (1999). For each value of coefficient of friction, models were run for the varying orientations of the far field stresses. As expected, increased friction along the faults tends to decrease the magnitude of the increased mean stress in the overstep region, as well as the size and extent of the region with the most stress change. The increased friction along the faults resists the shear stress that is resolved on the faults from the remote stress field, and therefore reduces slip on the faults. Once again using the case of a frictionless fault with $\theta = 30°$ as a base case, we see that with increasing friction along the fault, the interaction decreases dramatically until, at $\mu = 0.6$, slip is reduced almost completely and consequently there is virtually no interaction between the two segments (Fig. 8).

A convenient method to visualize the effect of varying

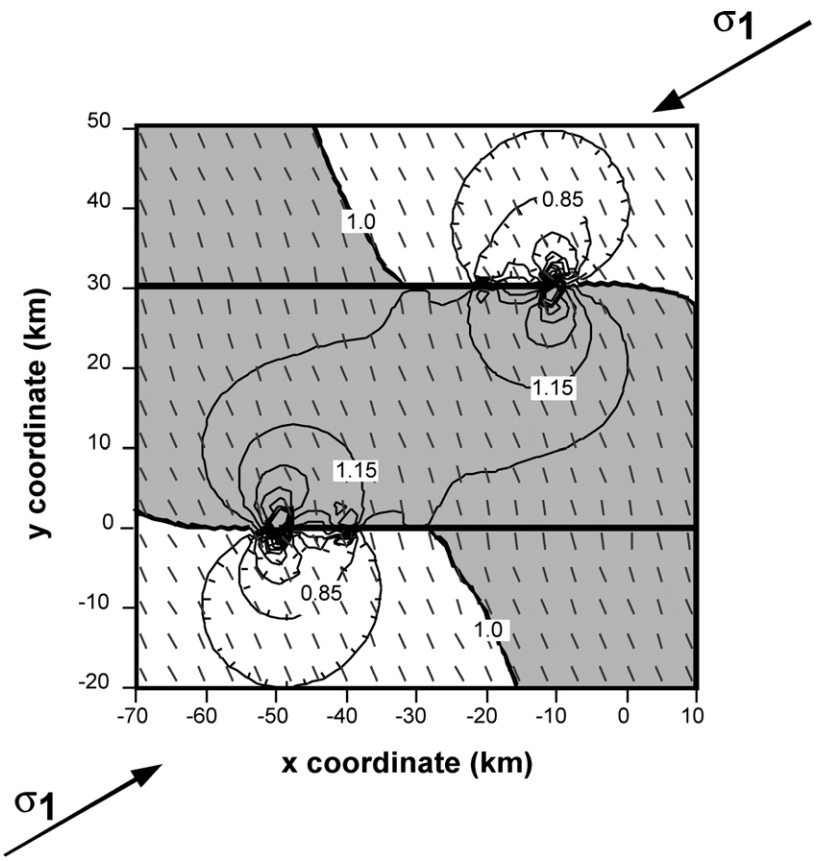

Fig. 6. Model results for base case model of frictionless faults and $\theta = 30°$. Plot shows both contours of mean stress $(\sigma_1 + \sigma_3)/2$ in overstep region and trajectories of planes on which the maximum compressive stress acts. Contour interval is 7.5% of remote mean stress. Values of mean stress are normalized to the far field value. Shaded area indicates region of increased mean stress. Note sharp increase in mean stress (increased compression) in the stepover. Orientation of planes is controlled primarily by orientation of far field stress, with local perturbations near the fault segments and their tip regions.

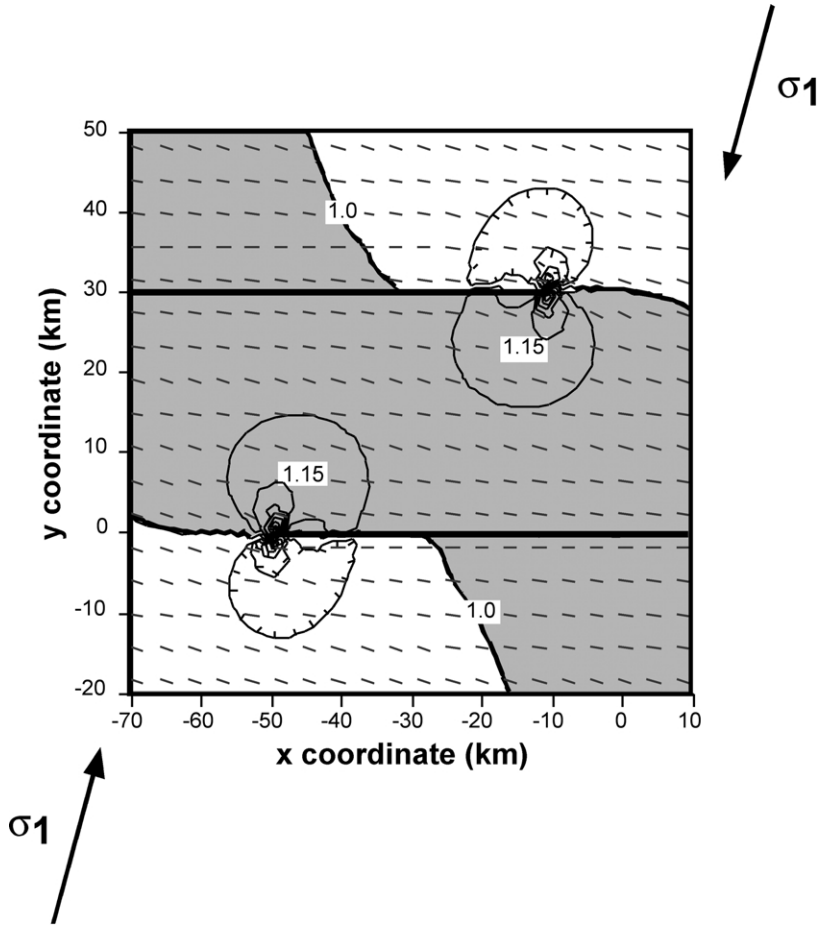

Fig. 7. Model results for frictionless faults and $\theta = 75°$. Contour interval is 7.5% of remote mean stress. Shaded area indicates region of increased mean stress. Increase in mean stress is much smaller than that in the $\theta = 30°$ base case. Trajectories of planes within the overstep region deviate slightly from being perpendicular to the far field stress orientation, becoming more parallel to the faults.

friction on the orientation of structures is to plot the computed strike of contractional structures with varying θ and μ at a particular location within the overstep zone. The model results for one location are shown in Fig. 9. It is apparent that the first order orientation of contractional structures is dependent on the far field stress orientations. However, it is also clear that friction along the bounding strike-slip faults does have an impact on the orientation of structures formed in the overstep region. Variations of up to nearly 10° are seen in some cases; in regions closer to the bounding faults, the variation can be even higher.

We also investigated the influence of $\sigma_1{:}\sigma_3$ stress ratios other than 5:1. Variation of this ratio did not impact the stress orientations in the fault overlap region, though the magnitude of the stress interaction was affected.

In comparing the model results with the structures in the field (i.e. the NW striking fault orientations), we are able to find a best match and consequently to make an estimate as to what boundary conditions were likely present at the time of deformation. A visual comparison with model outputs suggests that the best-fit model is that with very low fault frictions ($\mu = 0$ or 0.1) and with a remote stress field orientation of $\theta = 45°$ (see Fig. 10).

6. Discussion

At all scales, faults are commonly composed of numerous discrete segments which overlap in an en-échelon fashion and which mechanically interact. This characteristic of fault segmentation is commonly observed in dip-slip (normal and reverse faults) and oblique-slip faults as well as in strike-slip fault systems on a variety of scales, from centimeter- and meter-scale faults (Segall and Pollard, 1983) to regional (kilometer) scale transform plate boundaries (Aydin and Nur, 1982). Segmentation provides a primary control on the style and distribution of fault related deformation recognizable over a wide range of length scales.

Many workers have investigated échelon strike-slip fault segments using numerical models. Segall and Pollard (1980) provided a mechanical analysis of échelon fault segments by considering the stress interactions between two underlapping fault segments. Their results showed significant variations in mean stress and in maximum shear stress in the region between the two segments, with the sense of fault step and displacement controlling the stress distribution. Aydin and Schultz (1990) examined the self-similar

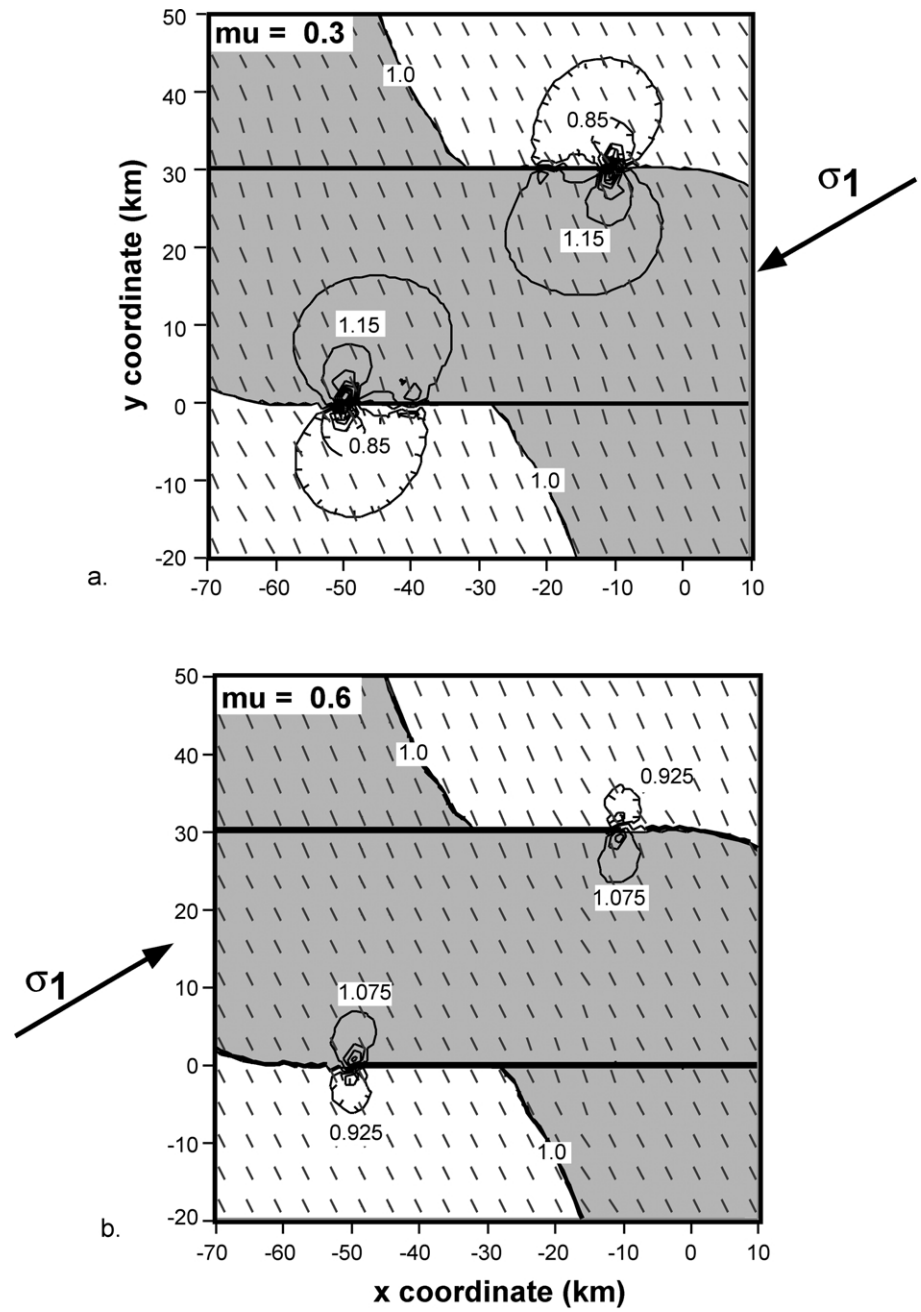

Fig. 8. Effect of increased friction on faults. $\theta = 30°$ for both cases; shaded area indicates region of increased mean stress. Contour interval is 7.5% of remote mean stress. (a) $\mu = 0.3$. Note reduced mean stress compared with frictionless case (see Fig. 6). (b) $\mu = 0.6$. Note dramatically reduced mean stress as compared with lower friction cases.

nature of segment overlap using a two-dimensional mechanical analysis of strike-slip fault segment pairs, and concluded that fault segment interaction enhances the tendency for fault growth as the fault segments approach each other, while this tendency is reduced after overlap is achieved, promoting échelon fault segment geometries. Ohlmacher and Aydin (1997) used two-dimensional numerical models to examine the variations in stress magnitudes and orientations with varying remote stress orientations and fault frictional properties. They found a wide variety of possible orientations of structures within fault overstep zones, and related these to different structures observed in the field.

Our numerical model results show conclusively that the increased compressive mean stress in the overstep zone between the strike-slip fault segments coincides with the region of contractional features, such as the large scale anticline and the reverse faults, identified in the field, as well as with the region of uplifted foreland that forms the Gargano block. Stress trajectories agree closely with the strike of the reverse or thrust faults, related folds, and tectonic pressure solution features. Stress trajectories

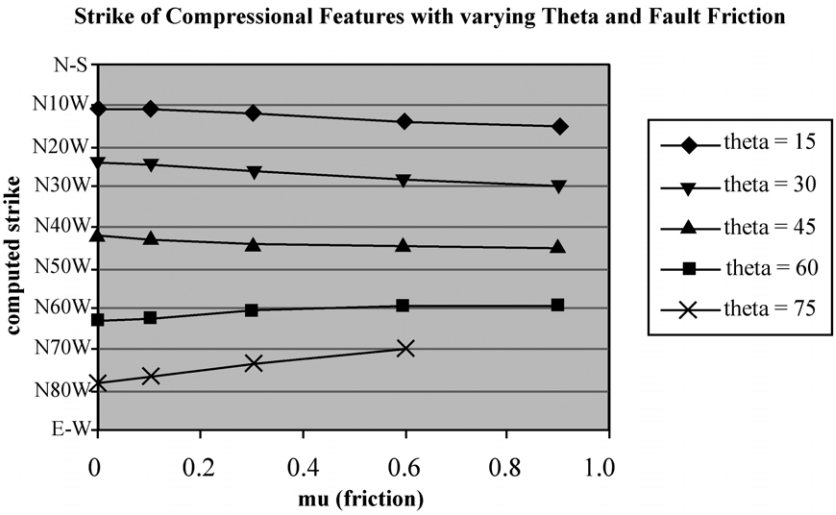

Fig. 9. Effect of varying stress orientation and fault friction on orientation of contractional structures at one location within the stepover zone. Remote stress orientation has primary control on structure orientation; friction has a smaller secondary effect, which can vary as much as 10°.

depend to the first order on the orientation of the remote stress field, while fault friction has a smaller effect on the orientations. A comparison of mapped structures with corresponding locations in the numerical models shows that the lower values of fault friction agree more closely with the observed data.

Furthermore, our analyses show that the cases of lower fault frictions ($\mu = 0.0$ and 0.1) produce a greater interaction between the boundary faults, and thus a greater perturbation in the mean stress, than higher values of fault friction. However, this does not in itself provide conclusive evidence for low friction faults. Our numerical models consider the effect of one 'pulse' of deformation, and do not consider the effect of multiple episodes superposed on one another. It is possible that repeated episodes of slip along the E–W-trending faults without stress relaxation could create the higher levels of compressive mean stress concentrated in the overstep zone that would cause uplift and deformation even for higher friction values.

However, the observation that many of the NW striking

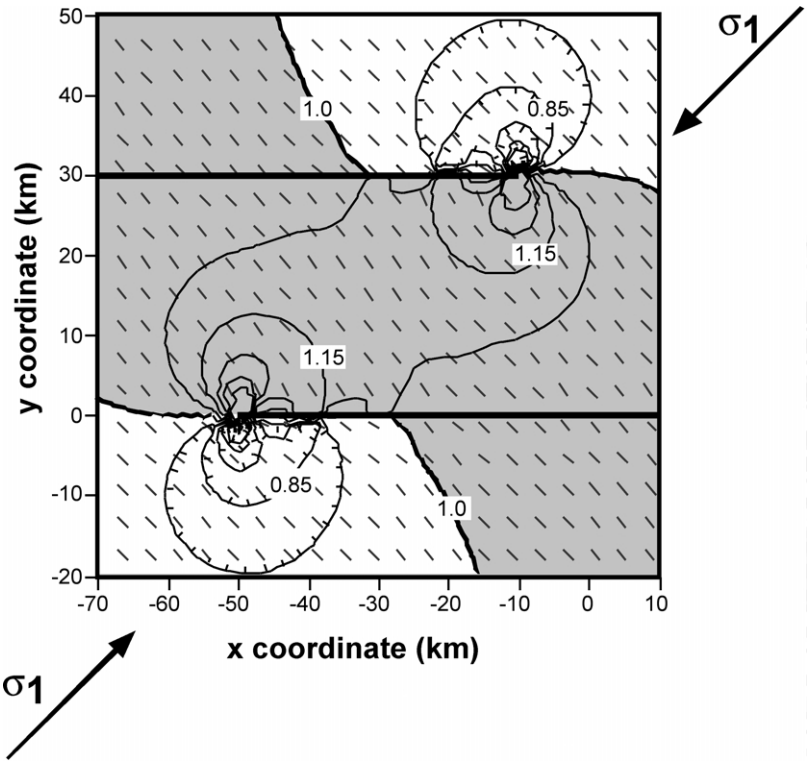

Fig. 10. Best fit match between field observations and model results. Fault friction is very low ($\mu = 0.1$) and $\theta = 45°$. Shaded area indicates region of increased mean stress.

faults terminate against the E–W-trending faults at high angles (see Fig. 2) correlates well with numerical models with low values of fault friction. This provides further evidence that the E–W-trending faults may have had low friction values during the deformation of the Gargano block. Conditions of low fault friction agree well with several studies on other strike-slip faults such as the San Andreas Fault in California, which proposed low values of fault friction (Mount and Suppe, 1987; Zoback et al., 1987).

Ohlmacher and Aydin (1997) examined the effects of friction and varying remote stress orientations on the local stress field in the vicinity of overlapping and parallel fault segments using a two-dimensional plane strain boundary element analysis. Their results show dramatic variations in the magnitude and orientations of principal stresses in the overstep regions between fault segments, depending on fault segment geometries and overlap configurations. Specifically, in contractional stepovers between fault segments, principal stress planes can vary as much as 30° from the remote stress orientations, depending mainly on fault friction. Our analyses, however, indicate that stress orientations in the overstep zone depend to first order on the remote stress orientations, and only to a minor amount on fault friction (Fig. 9), with the exception of the region extremely close to the fault segments.

The difference between the two results lies in the nature of two-dimensional versus three-dimensional analysis. By definition, two-dimensional vertical faults are infinitely tall and every horizontal plane of observation provides the same stress concentration and orientations. In contrast, three-dimensional modeling allows us to incorporate the actual height of the modeled faults in the analysis. Since the height of the faults in our models is relatively short with respect to the lateral dimensions of the overstep region and the length of the fault segments, there is relatively little interaction between the échelon faults, and consequently a minor effect on the orientation of the stress field in the overlap area. Had our modeled faults been taller (i.e. >10 km), an increased effect on stress magnitude and orientations in the overstep zone would have resulted.

In order to assess this effect, we ran additional models with varying fault height and compared the stress perturbations and the orientations of potential contractional structures from the different models. As shown by Fig. 11a, models incorporating unrealistically tall faults (e.g. 100 km in vertical dimension) show dramatically increased compressive stress within the stepover zone, with stress increases of up to 37% in the center of the stepover, as opposed to about 7.5% in the model with 10 km high faults (see Fig. 6). Orientation of the principal stresses, and thus the resulting contractional structures, also varies as a function of fault height. For each fault height, orientations vary by up to 25° from the far-field stress, depending on the location within the stepover region (see Fig. 11b). As the faults become taller, the principal stress orientations at each point approach the values found by two-dimensional models, such as those by Ohlmacher and Aydin (1997). These model results indicate that the height of the faults exerts a primary control on the orientations of structures developing within the stepover zone. In addition, if the overlap between the fault segments had been larger, and/or the separation been smaller, an increased interaction between fault segments would have occurred. Given such a dominant effect of fault height, the depth of the strike-slip faults in our models becomes important. Fortunately, the existence of seismic data provides well-constrained fault heights for the Mattinata fault, the best known of the E–W-trending strike-slip faults. Marine seismic data show a vertical dimension of at least 10 km for this fault (Finetti et al., 1987; de Alteriis and Aiello, 1993; Argnani et al., 1993).

Since numerous smaller E–W striking fault segments are present in the overstep region, it is likely that these faults, too, had an effect during the uplift of the Gargano block. During the initial stages of deformation, these smaller faults may have interacted with the major bounding faults, resulting in sub-areas of local uplift deformation, as evident from small connecting faults joining the smaller E–W faults. As deformation progressed, slip was concentrated along the major strike-slip faults, and these became the bounding structures of the uplift region with the majority of the uplift localized across them. The presence of E–W faults (e.g. Rignano Fault) and a NW-trending oblique reverse fault (Candalero Fault) south of the main southern boundary fault support this view that deformation may have started in a broad zone and nucleated inward to the main zone of uplift.

6.1. Timing of deformation and inversion of prior structures

Determination of the timing and duration of the uplift deformation in the Gargano Promontory is difficult due to the lack of correlatible stratigraphy across the major strike-slip faults and the lack of younger deposits to constrain the end of deformation. We can estimate the onset of deformation as being upper Miocene or later due to the involvement of Miocene strata in the faulting. This coincides approximately with the onset of thrusting in the Apennines to the west, and the direction of compression in the Apennines is consistent with that which caused displacement on the strike-slip faults in the Gargano. Timing of the end of deformation is unconstrained, though it is likely that the deformation extended into at least the Pliocene. The presence of possible Pleistocene marine terraces along the eastern coast of the Gargano indicates that uplift may have continued, though the low elevations of the possible terraces indicate much slower uplift. We have no data on possible rates of deformation or uplift in the Pleistocene.

It should be noted that the strike of the reverse faults in the Gargano is very similar to the strike of the regional-scale normal faults present throughout the rest of the Apulian

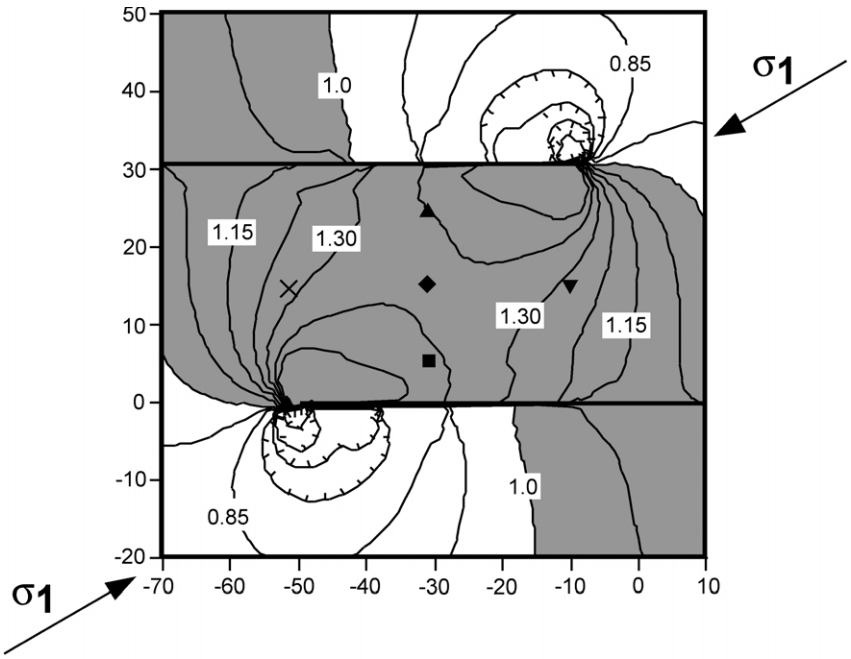

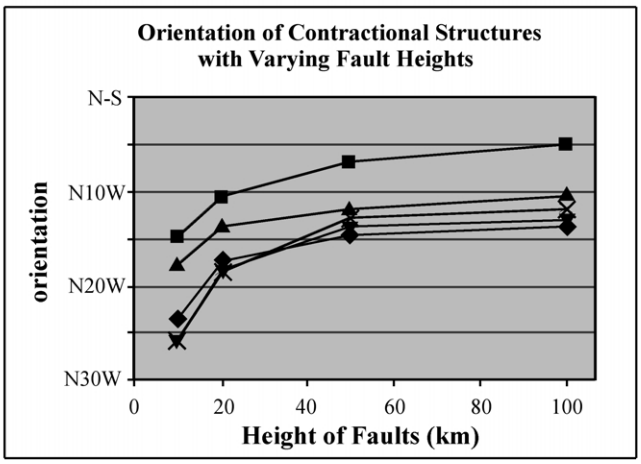

Fig. 11. Effect of fault height on stress perturbation and orientations of the contractional structures. $\theta = 30°$ for both cases; shaded area indicates region of increased mean stress. (a) Contours of mean stress for 100-km-high faults. Note dramatically increased mean stress in stepover region compared with 10-km-high fault case (see Fig. 6). (b) Orientation of contractional structures at various locations with different fault heights. Orientations with increasing fault height vary up to 25° from the far-field orientation, depending on modeled fault heights. Symbols refer to different locations in (a).

foreland. In many cases, the reverse faults are relatively high-angle (dips of 40–60°; Fig. 4). In addition, some NW-striking normal faults are present in the northeast portion of the Gargano. It is likely, then, that the localized compression in the Gargano block caused the reactivation of pre-existing normal faults as reverse faults.

6.2. Application to the southern Apennines

The presence within the foreland block of a structural domain characterized by contractional deformation and uplift draws the question of whether similar regions might exist where localized contractional deformation is present in the midst of a different, and possibly more complicated, tectonic setting This style of deformation was described in detail by Campagna and Aydin (1991) with the uplift of the Echo Hills within the southern Basin and Range Province. In that case, shortening and uplift within the otherwise regional extension is localized between overstepping strike-slip fault segments. This is similar to the mechanism that we propose for the Gargano.

Similar deformational styles are present in the more complexly deformed interior of the southern Apennines, both at the surface and in the subsurface (Monaco et al., 1998; Cello and Mazzoli, 1999). Monaco et al. (1998) reported several surface exposures where a series of reverse faults are localized between a series of left-lateral strike-slip faults (Fig. 12a). In some cases, uplift along these strike-slip faults and the related thrust faults is sufficient for Apulian carbonate units from the footwall

of the thrust system to be exposed at the surface, for example, in the regions of Monte Alpi and Pollino (Catalano et al., 1993; Monaco, 1993). For this to occur, these units would have to have been uplifted through several thousand meters of overlying allochthonous units. Uplift of this magnitude occurs only in the localized regions between overlapping strike-slip faults, and indicates that this mechanism of uplift is capable of producing large (kilometer scale) vertical displacements. This style of deformation is identical to that which we propose as the mechanism for the Gargano uplift.

Fig. 12b shows a subsurface example from a hydrocarbon reservoir located at depth in the overthrusted Apulian platform carbonates in the southern Apennines, Italy. The reservoir is located at a structural high localized at a compressive step in a strike-slip fault, similar in structural style to the Gargano (Mobil Oil Italiana, pers. com.). Of interest in this example is the fact that the reservoir structure is located within the stratigraphically equivalent units to those in the Gargano. While the scale of this reservoir structure is smaller than the surface case of the Gargano, the kinematic and mechanical relationships between the primary structures and the deformation is essentially identical. The fact that this style is present at locations within the southern Apennines, both at the surface and at depth, indicates that the concept of this structural style in the defining of potential hydrocarbon targets may be important in the exploration and definition of economically significant resources.

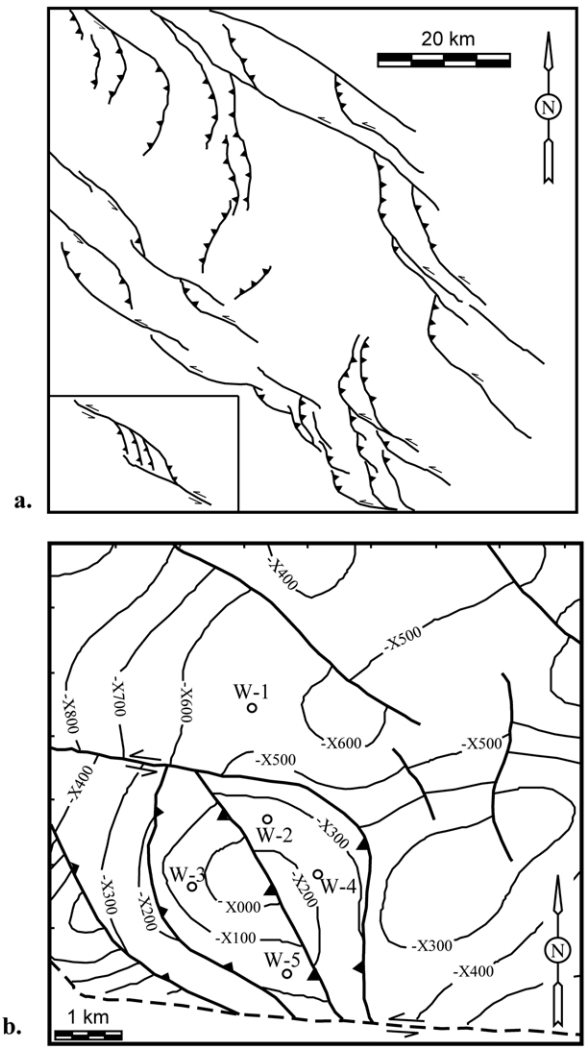

Fig. 12. (a) Fault map of portion of southern Apennines (after Monaco et al., 1998) showing relationships between strike-slip fault system and reverse faults occurring at contractional stepovers. (b) Structure map from a hydrocarbon reservoir in the southern Apennines, Italy. Contours are of a prominent stratigraphic surface and are in meters (negative sign indicates elevation below sea level); the precise elevations have been concealed due to data confidentiality. Structural high is located at contractional step along nearly E–W strike-slip fault system. Other faults at high angles to the E–W faults are most likely reverse faults. Note similar relative fault orientation in both (a) and (b) to fault pattern in the Gargano Promontory.

7. Conclusions

We have identified two regional-scale E–W-trending right-stepping, left-lateral strike-slip fault zones which bound the Gargano block on the south and the north. Within this uplifted push up block of the Apulian foreland, NW-striking contractional structures are pervasive. We propose that the origin of the compressional stresses responsible for the observed uplift and contractional deformation (i.e. folding, reverse faulting, and pressure solution) is the interaction between the two bounding fault zones. Three-dimensional numerical models incorporating the observed geometry of and slip sense across the boundary faults with reasonable remote stresses lend support for this interpretation. Consideration of this mechanism of uplift may be important for the interpretation of local structural styles in other regions of the foreland, and for interpreting the subsurface deformational history of the overthrusted Apulian units in the southern Apennines.

In addition, the model study presented here highlights significant differences between results from earlier two- and three-dimensional half-space models. In this respect, this study shows that care should be taken in using two-dimensional models for three-dimensional fault studies.

Acknowledgements

This work was supported by a National Science Foundation Graduate Student Fellowship, a grant from Mobil Oil Italiana, and the Stanford Rock Fracture Project. Additional logistical support from Mobil Oil Italiana for the fieldwork is gratefully acknowledged. Constructive and detailed reviews by Francesco Salvini, Giuseppe Cello, and Tom Blenkinsop greatly improved the manuscript. Discussions with Laird Thompson, Jim Carpenter, and Peter Hennings strengthened several ideas contained in this

contribution. Thanks to Scott Young and Laurent Maerten for assistance with Poly3D, to Andrea Billi for stimulating and helpful discussions and logistical support, and to Paolo Zambianchi for fieldwork assistance.

References

de Alteriis, G., Aiello, G., 1993. Stratigraphy and tectonics offshore of Puglia (Italy, southern Adriatic Sea). Marine Geology 113, 233–253.

Amato, A., Montone, P., Casero, M., 1995. State of stress in southern Italy from borehole breakout and focal mechanism data. Geophysical Research Letters 22, 3119–3122.

Argnani, A., Favali, P., Frugoni, F., Gasperini, M., Ligi, M., Marani, M., Mattietti, G., Mele, G., 1993. Foreland deformational pattern in the southern Adriatic Sea. Annali di Geofisica 36, 229–247.

Aydin, A., Nur, A., 1982. Evolution of pull-apart basins and their scale independence. Tectonics 1, 91–105.

Aydin, A., Schultz, R.A., 1990. Effect of mechanical interaction on the development of strike-slip faults with echelon patterns. Journal of Structural Geology 12, 123–129.

Aydin, A., Schultz, R.A., Campagna, D., 1990. Fault-normal dilation in pull-apart basins; implications for the relationship between strike-slip faults and volcanic activity. Annales Tectonicae 4, 45–52.

Bigazzi, G., Laurenzi, M.A., Principe, C., Brocchini, D., 1996. New geochronologic data on igneous rocks and evaporites of the Pietre Nere point (Gargano Peninsula, southern Italy). Bolletino della Societa Geologica Italiana 115, 439–448.

Billi, A., 2003. Solution slip and separations on strike-slip fault zones: theory and application to the Mattinata fault, Italy. Journal of Structural Geology 25, 703–715.

Boni, A., Bruno, G., Casnedi, R., Centamore, E., Colantoni, P., Cremonini, G., Elmi, C., Monesi, A., Motta, E., Perotto, G., Valletta, M., 1969. Carta geologica d'Italia alla scala 1:100,000, foglio 155, San Severo. Servizio Geologica d'Italia, Rome.

Campagna, D.J., Aydin, A., 1991. Tertiary uplift and shortening in the Basin and Range; the Echo Hills, southeastern Nevada. Geology 19, 485–488.

Cassano, E., Fichera, R., Arisi Rota, F., 1986. Rilievo aeromagnetico d'Italia. Alcuni risultati interpretativi. In: Proceedings of the 5th Meeting, Gruppo Nazionale di Geofisica della Terra Solida, CNR, Rome, pp. 939–958.

Catalano, S., Monaco, C., Tortorici, L., Tansi, C., 1993. Pleistocene strike-slip tectonics in the Lucanian Apennine (Southern Italy). Tectonics 12, 656–665.

Cello, G., Mazzoli, S., 1999. Apennine tectonics in southern Italy: a review. Journal of Geodynamics 27, 191–211.

Cello, G., Tortorici, L., Martini, N., Paltrinieri, W., 1989. Structural styles in the frontal zones of the southern Apennines, Italy: an example from the Molise district. Tectonics 8, 753–768.

Channel, J., D'Argenio, B., Horvath, F., 1979. Adria, the African Promontory, in Mesozoic Mediterranean palaeogeography. Earth-Science Reviews 15, 213–292.

Console, R., Di Giovambattista, R., Favali, P., Presgrave, B.W., Smriglio, G., 1993. Seismicity of the Adriatic microplate. Tectonophysics 218, 343–354.

Cremonini, G., Emli, C., Selli, R., 1971. Carta geologica d'Italia alla scala 1:100,000, foglio 156, S. Marco in Lamis. Servizio Geologica d'Italia, Rome.

Crider, J.G., Pollard, D.D., 1998. Fault linkage: three-dimensional mechanical interaction between echelon normal faults. Journal of Geophysical Research 103, 24373–24391.

de Dominicis, A., Mazzoldi, G., 1987. Interpretazione geologico-stutturale del margine orientale della piattaforma Apula. Memorie della Societa Geologica Italiana 38, 163–176.

Favali, P., Mele, G., Mattietti, G., 1990. Contribution to the study of the Apulian microplate geodynamics. Memorie della Societa Geologica Italiana 44, 71–80.

Favali, P., Funiciello, R., Mattietti, G., Mele, G., Salvini, F., 1993a. An active margin across the Adriatic Sea (central Mediterranean Sea). Tectonophysics 219, 109–117.

Favali, P., Funiciello, R., Salvini, F., 1993b. Geological and seismological evidence of strike-slip displacement along the E–W Adriatic-central Apennine belt. In: Boschi, E., Mantoroni, E., Morelli, A. (Eds.), Recent Evolution and Seismicity of the Mediterranean Region, Kluwer Academic Publishers, pp. 333–346.

Finetti, I., Morelli, C., 1973. Geophysical exploration of the Mediterranean Sea. Bollettino di Geofisica Teorica ed Applicata 15, 263–341.

Finetti, I., Bricchi, G., del Ben, A., Pipan, M., Xuan, Z., 1987. Geophysical study of the Adria plate. Memorie della Societa Geologica Italiana 40, 335–344.

Fletcher, R., Pollard, D.D., 1981. Anticrack model for pressure solution surfaces. Geology 9, 419–424.

Funiciello, R., Montone, P., Salvini, F., Tozzi, M., 1988. Caratteri strutturali del promontorio del Gargano. Memorie della Societa Geologica Italiana 41, 1235–1243.

Funiciello, R., Montone, P., Parotto, M., Salvini, F., Tozzi, M., 1991. Geodynamical evolution of an intra-orogenic foreland: the Apulia case history (Italy). Bollettino della Societa Geologica Italiana 110, 419–425.

Kattenhorn, S.A., Pollard, D.D., 1999. Is lithostatic loading important for the slip behavior and evolution of normal faults in the Earth's crust? Journal of Geophysical Research 104, 28879–28898.

Lavecchia, G., 1988. The Tyrrhenian–Apennines system: structural setting and seismotectogenesis. Tectonophysics 147, 263–296.

Maerten, L., Willemse, E.J.M., Pollard, D.D., Rawnsley, K., 1999. Slip distributions on intersecting normal faults. Journal of Structural Geology 21, 259–271.

Marsella, E., Bally, A.W., Cippitelli, G., D'Argenio, B., Pappone, G., 1995. Tectonic history of the Lagonegro Domain and Southern Apennine thrust belt evolution. Tectonophysics 252, 307–330.

Martinis, B., Pavan, G., 1967. Carta geologica d'Italia alla scala 1:100,000, foglio 157, Monte S. Angelo. Servizio Geologica d'Italia, Rome.

Merla, G., Ercoli, A., Torre, D., 1969. Carta geologica d'Italia alla scala 1:100,000, foglio 164, Foggia. Servizio Geologica d'Italia, Rome.

Monaco, C., 1993. Pleistocene strike-slip tectonics in the Pollino mountain range (southern Italy). Annales Tectonicae 7, 100–112.

Monaco, C., Tortorici, L., Paltrinieri, W., 1998. Structural evolution of the Lucanian Apennines, southern Italy. Journal of Structural Geology 20, 617–628.

Mount, V.S., Suppe, J., 1987. State of stress near the San Andreas Fault: implications for wrench tectonics. Geology 15, 1143–1146.

Ohlmacher, G.C., Aydin, A., 1997. Mechanics of vein, fault, and solution surface formation in the Appalachian Valley and Ridge, northeastern Tennessee, USA: implications for fault friction, state of stress, and fluid pressure. Journal of Structural Geology 19, 927–944.

Ortolani, F., Pagliuca, S., 1987. Tettonica transpressiva nel Gargano e rapporti con le catene Appenninica e Dinarica. Memorie della Societa Geologica Italiana 38, 205–224.

Patacca, E., Scandone, P., 1989. Post-Tortonian mountain building in the Apennines. The role of the passive sinking of a relci lithospheric slab. In: Boriani, A., Bonafede, M., Piccardo, G.B., Vai, G.B. (Eds.), The Lithosphere in Italy, Accademia Nazionale dei Lincei, pp. 157–176.

Patacca, E., Sartori, R., Scandone, P., 1990. Tyrrhenian basin and Apenninic arcs: kinematic relations since late Tortonian times. Memorie della Societa Geologica Italiana 45, 425–451.

Salvini, F., Funicello, R., 1994. Rigetti stratigraphici e rigetti reali: il paradosso apparente della faglia di Mattinata (Gargano). In: Societa Geologica Italiana 77 Riunione estiva, Congresso Nazionale, Bari.

Salvini, F., Billi, A., Wise, D.U., 1999. Strike-slip fault-propagation cleavage in carbonate rocks: the Mattinata Fault zone, Southern Apennines, Italy. Journal of Structural Geology 21, 1731–1749.

Segall, P., Pollard, D.D., 1980. Mechanics of discontinuous faults. Journal of Geophysical Research 85, 4337–4350.

Segall, P., Pollard, D.D., 1983. Nucleation and growth of strike-slip faults in granite. Journal of Geophysical Research 88, 555–568.

Thomas, A.L., 1993. Poly3D: a three-dimensional, polygonal element, displacement discontinuity boundary element computer program with applications to fractures, faults, and cavities in the Earth's crust. M.S. thesis, Stanford University.

Willemse, E.J.M., Pollard, D.D., Aydin, A., 1996. Three-dimensional analyses of slip distributions on normal fault arrays with consequences for fault scaling. Journal of Structural Geology 18, 295–309.

Zoback, M.D., Zoback, M.L., Mount, V.S., Suppe, J., Eaton, J.P., Healy, J.H., Oppenheimer, D., Reasenberg, P., Jones, L., Raleigh, C.B., Wong, I.G., Scotti, O., Wentworth, C., 1987. New evidence on the state of stress of the San Andreas Fault system. Science 238, 1105–1111.